

FASTERD: a Monte Carlo event generator for the study of final state radiation in the process $e^+e^- \rightarrow \pi\pi\gamma$ at DAΦNE

O. Shekhovtsova^{a,b,1}, G. Venanzoni^a, G. Pancheri^a

^a*INFN Laboratori Nazionale di Frascati, Frascati (RM) 00044, Italy*

^b*NSC KIPT, Kharkov 61202, Ukraine*

Abstract

FASTERD is a Monte Carlo event generator to study the final state radiation both in the $e^+e^- \rightarrow \pi^+\pi^-\gamma$ and $e^+e^- \rightarrow \pi^0\pi^0\gamma$ processes in the energy region of the ϕ -factory DAΦNE. Differential spectra that include both initial and final state radiation and the interference between them are produced. Three different mechanisms for the $\pi\pi\gamma$ final state are considered: Bremsstrahlung process (both in the framework of sQED and Resonance Perturbation Theory), the ϕ direct decay ($e^+e^- \rightarrow \phi \rightarrow (f_0; f_0 + \sigma)\gamma \rightarrow \pi\pi\gamma$) and the double resonance mechanism (as $e^+e^- \rightarrow \phi \rightarrow \rho^\pm\pi^\mp \rightarrow \pi^+\pi^-\gamma$ and $e^+e^- \rightarrow \rho \rightarrow \omega\pi^0 \rightarrow \pi^0\pi^0\gamma$). Additional models can be incorporated as well.

PACS: 13.25.Jx; 12.39.Fe; 13.40.Gp.

Key words: Quantum electrodynamics (QED), e^+e^- -annihilation, hadronic cross section, radiative corrections, low energy photon-pion interaction model

PROGRAM SUMMARY

Program Title: FASTERD

Authors: G. Pancheri, O. Shekhovtsova, G. Venanzoni

Journal Reference:

Catalogue identifier:

Licensing provisions: none

Programming language: FORTRAN77

Computer: any computer with FORTRAN77 compiler

Operating system: UNIX, LINUX, MAC OSX

¹ Corresponding author

Keywords: Quantum electrodynamics (QED), e^+e^- -annihilation, hadronic cross section, radiative corrections, low energy photon-pion interaction model.

PACS: 13.25.Jx; 12.39.Fe; 13.40.Gp.

Classification: 11.1

External routines/libraries: MATHLIB, PACKLIB from CERN library

Nature of problem: General parameterization of the $\gamma^* \rightarrow \pi\pi\gamma$ process; test models describing Bremsstrahlung process, the ϕ direct decay, double vector resonance mechanism.

Solution method: Numerical integration of analytical formulae

Restrictions: Only one photon emission is considered

Running time 28 sec with standard input card (1e6 events generated) on a Intel Core 2 Duo 2. GHz with 1 GB RAM.

1 Introduction

The anomalous magnetic moment of the muon (a_μ) is one of the most precise test of the Standard Model [1]. Theoretical predictions differ from the experimental result for more than 3σ [2]. The main source of uncertainty in the theoretical prediction comes from the hadronic contribution, $a_\mu^{(had)}$ [2]. This contribution cannot be reliably calculated in the framework of perturbative QCD (pQCD), because low-energy region dominates, but it can be estimated by dispersion relation using the experimental cross sections of e^+e^- annihilation into hadrons as an input [3]. About 70% of the hadronic part of the muon anomalous magnetic moment, $a_\mu^{(had)}$, comes from the energy region below 1 GeV and, due to the presence of the ρ -meson, the main contribution to $a_\mu^{(had)}$ is related with the $\pi^+\pi^-$ final state.

Experimentally, the energy region from threshold to the collider beam energy is explored at the Φ -factory DAΦNE, *PEP-II* and *KEKB* at $\Upsilon(4S)$ -resonance using the method of radiative return (for a review see [4] and references therein). This method relies on the factorization of the radiative cross section into the product of the hadronic cross section times a radiation function $H(q^2, \theta_{max}, \theta_{min})$ known from Quantum Electrodynamics (QED) [5,6,7,8,9]. For two pions final state it means that, in the presence of only the initial state radiation (by leptons, ISR), the radiative cross section $\sigma^{\pi\pi\gamma}$ corresponding to the process

$$e^+(p_+) + e^-(p_-) \rightarrow \pi^+(p_1) + \pi^-(p_2) + \gamma(k), \quad (1)$$

can be written as $d\sigma^{\pi\pi\gamma} = d\sigma^{\pi\pi}(q^2)H(q^2, \theta_{max}, \theta_{min})$ [4,7,9], where θ_{min} and θ_{max} are the minimal and maximal azimuthal angles of the radiated photon, $q = p_1 + p_2$ and the hadronic cross section $\sigma^{\pi\pi}$ is taken at a reduced CM energy. The final state (FS) radiation (FSR) is an irreducible background in radiative return measurements of the hadronic cross section [7,10] and spoils the factorization of the cross section. In any experimental setup the process of FSR cannot be excluded from the analysis. The KLOE experiment has developed two different analysis strategies: the first one is with the photon emitted at small angle ($\theta_\gamma < 15^\circ$) and the other one is for the photon reconstructed at large angle ($60^\circ < \theta_\gamma < 120^\circ$), being for both $50^\circ < \theta_\pi < 130^\circ$. In the case of the small angle kinematics the FSR contribution can be safely neglected, while for the large angle analysis it becomes relevant (upto 40% of ISR). The large angle analysis allows to scan the pion form factor down to the threshold [11].

Radiative corrections (RC's) related to initial state radiation, i.e. the function H , can be safely computed in QED. For the FSR process the situation is different. In the region below 2 GeV the pQCD is not applicable to describe FSR and calculation of the cross section relies on the low energy pion-photon inter-

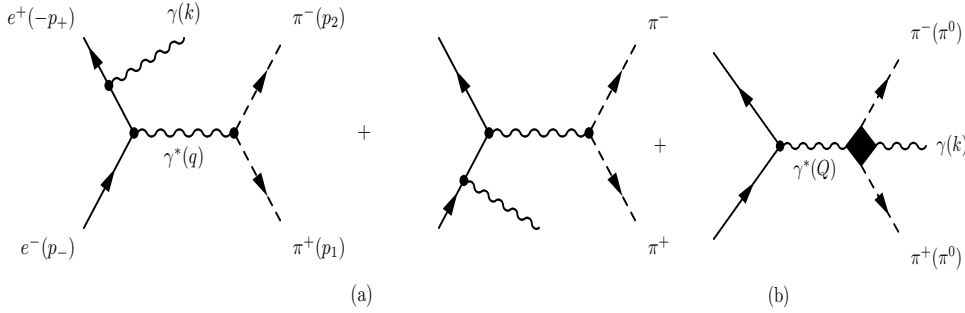


Fig. 1.

action model. Thus the measured FSR cross section gives an unique possibility to get very interesting information on the dynamics of interacting mesons and photons, to test the pion-photon interaction models and extract their parameters [12].

In the case of neutral pions in the final states

$$e^+(p_+) + e^-(p_-) \rightarrow \pi^0(p_1) + \pi^0(p_2) + \gamma(k), \quad (2)$$

the ISR contribution is absent², and the cross section is determined solely by the FSR mechanism. This process, together with asymmetries [13] and cross section in the charged channel, allows to extract information on pion-photon interaction and test effective models for FSR.

For realistic experimental cuts on the angle and energy of the final particles the cross section cannot be evaluated analytically and one has to use Monte Carlo (MC) event generator. The first MC describing the reaction (1) was EVA [7]. EVA simulates both ISR and FSR processes for non zero angle emitted photon ($\theta_\gamma > \theta_{min}$). For FSR the sQED model was chosen. Afterwards the MC PHOKHARA was written to include different charged final state and radiative corrections to ISR [14]. The contribution of the ϕ -meson direct decay, that is relevant at the DAΦNE energy, was added, firstly in EVA [15] and then in PHOKHARA [13].

The computer code FASTERD³ presented in this paper is a Monte Carlo event generator written in FORTRAN that simulates both processes (1) and (2), where the hard photon $\gamma(k)$ can be emitted by the leptons⁴ and/or the pions Fig. 1. This program was inspired by EVA. The present version of FASTERD includes different mechanisms for the $\pi\pi\gamma$ production: final Bremsstrahlung⁵ in the framework of both Resonance Perturbation Theory and sQED, the con-

² This statement is valid only if one neglects multi-photon emission

³ FinAL StatE Radiation at DAΦNE

⁴ Only for the charged channel

⁵ Only for the charged channel

tributions related to the ϕ intermediate state and the double vector resonance part (for details see Section 3). Up to now only the case of one photon emission has been considered. The code contains two types of source files: (1) the main program **fasterd.f**, where the calculations are done, and (2) the input file **cards_fasterd.dat** which defines the parameters for the generation. Both these files will be described in the following. As output of the program, the cross section of the process is evaluated and a PAW/HBOOK ntuple is produced with the 4-momenta for each event of the outgoing particles. For the convenience of the user we have added a Makefile and the test output files for the Journal library.

This paper is organized as follows. In Section 2 the main formulae for ISR and interference between ISR and FSR are presented. In Section 3 we give a general description of FSR process and present the FSR models that are included in our program. In Section 4 the spectra for different FSR models are compared with analytical results and with MC PHOKHARA. Also a possible generalization applicable to a wider region is described in Section 4. In Section 5, we summarize the general procedure for calculating the spectrum. In Appendices A, B, C a short description of the input and output files is presented.

2 Initial state radiation models and pion form factor

The cross section of the processes (1) and (2) can be written as

$$\begin{aligned} d\sigma &= \frac{1}{2s(2\pi)^5} C_{12} \int \delta^4(Q - p_1 - p_2 - k) \frac{d^3p_1 d^3p_2 d^3k}{8E_+ E_- \omega} |M|^2 \\ &= C_{12} N |M|^2 dq^2 d\Omega' d\Omega^{\pi^+}, \quad \left(N = \frac{\alpha^3 (s - q^2)}{64\pi^2 s^2} \sqrt{1 - \frac{4m_\pi^2}{q^2}} \right) \end{aligned} \quad (3)$$

where α is the fine structure constant, m_π is the pion mass, ω is the photon energy, $Q = p_+ + p_-$, $s = Q^2$ and the invariant amplitude squared, averaged over initial lepton polarizations and summed over the photon polarizations⁶ is

$$\overline{|M|^2} = \overline{|M_{ISR}|^2} + \overline{|M_{FSR}|^2} + 2\text{Re}(\overline{M_{ISR} M_{FSR}^*}). \quad (4)$$

$M^{(ISR)}$ ($M^{(FSR)}$) corresponds to the ISR(FSR) production amplitude. The factor $C_{12} = \frac{1}{2}$ for $\pi^0\pi^0$ in the final state and $C_{12} = 1$ for $\pi^+\pi^-$.

⁶ We use $\sum_{polar.} \epsilon_\rho^* \epsilon_\sigma = -g_{\rho\sigma}$

For ISR process the invariant amplitude squared, averaged over initial lepton polarizations and summed over the photon polarizations, is

$$\begin{aligned} \overline{|M^{(ISR)}|^2} &= -\frac{4}{q^2} |F_\pi(q^2)|^2 R, \\ R &= \frac{m_\pi^2}{q^2} F + \frac{\chi_1^2 + \chi_2^2 - \chi_1(q^2 - t_2) - \chi_2(q^2 - t_1)}{t_1 t_2} \\ &\quad - \frac{2m_e^2 \chi_1}{t_2^2} \left(\frac{\chi_1}{q^2} - 1 \right) - \frac{2m_e^2 \chi_2}{t_1^2} \left(\frac{\chi_2}{q^2} - 1 \right), \quad F = \frac{(q^2 - t_1)^2 + (q^2 - t_2)^2}{t_1 t_2}, \end{aligned} \quad (5)$$

where m_e is the electron mass, $\chi_{1,2} \equiv 2p_{-,+} \cdot p_2$, $t_1 = -2p_- k$, $t_2 = -2p_+ k$.

The nonpoint-like behaviour of pions is determined by the form-factor (FF) $F_\pi(q^2)$ that is the function of the pion mass squared q^2 . In the case of the neutral channel $M^{(ISR)} = 0$. Four different parameterizations for the pion FF are considered: Kühn-Santamaria (KS) [16], Gounaris-Sakurai (GS) [17], the RPT parametrization and an "improved" version of Kühn-Santamaria (see below) [18].

2.1 Kühn-Santamaria and Gounaris-Sakurai pion FF

Based on the results of Ref. [16], the pion FF describing the $\rho - \omega$ mixing and the first excited ρ resonance (ρ'), can be written as

$$F_\pi(q^2) = \frac{B_\rho \frac{1+\alpha B_\omega}{1+\alpha} + \beta B_{\rho'}}{1 + \beta}, \quad (6)$$

where for the KS parametrization [16]

$$B_r^{KS}(q^2) = \frac{m_r^2}{m_r^2 - q^2 - i\sqrt{q^2}\Gamma_r(q^2)} \quad (7)$$

and for the GS one [17]

$$B_r^{GS}(q^2) = \frac{m_r^2 + H(0)}{m_r^2 - q^2 + H(q^2) - i\sqrt{q^2}\Gamma_r(q^2)}, \quad (8)$$

with

$$H(q^2) = \frac{m_\rho^2 \Gamma_\rho}{p_\pi^3(m_\rho^2)} \left[p_\pi^2(q^2)(h(q^2) - h(m_\rho^2)) + (m_\rho^2 - q^2) p_\pi^2(m_\rho^2) \frac{dh}{dq^2} \Big|_{q^2=m_\rho^2} \right],$$

$$h(q^2) = \frac{2}{\pi} \frac{p_\pi(q^2)}{\sqrt{q^2}} \ln \frac{\sqrt{q^2} + 2p_\pi(q^2)}{2m_\pi}, \quad p_\pi(q^2) = \frac{1}{2} \sqrt{q^2 - m_\pi^2}.$$

The energy dependence for the ρ mesons is taken in the form

$$\Gamma_\rho(q^2) = \Gamma_\rho \frac{m_\rho^2}{q^2} \left(\frac{p_\pi(q^2)}{p_\pi(m_\rho^2)} \right)^3 \cdot \Theta(q^2 - 4m_\pi^2). \quad (9)$$

For the ω resonance a simple Breit-Wigner resonance form with constant width was used for both parameterizations.

As one can see the single resonance contribution is normalized to unity at $q^2 = 0$ for both parameterizations ($B_r(0) = 1$) whereas the right normalization for the pion FF, $F_\pi(0) = 1$, is realized by the corresponding choice of the parameters α, β .

All model parameters (the mass and width of the resonances as well as the parameter α, β) are determined in the input file **cards_fasterd.dat**. The KS pion FF parametrization corresponds to the function **F_pi_ks** whereas the GS one to **F_pi_gs**.

2.2 RPT parametrization for the pion FF

The Resonance Perturbation Theory is based on Chiral Perturbation Theory (χ PT) with the explicit inclusion of the vector and axial-vector mesons, $\rho_0(770)$ and $a_1(1260)$. Whereas χ PT gives correct predictions for the pion form factor at very low energy, RPT is the appropriate framework to describe the pion form factor at intermediate energies ($E \sim m_\rho$) [19]. According to the RPT model the pion form factor, that describes the $\rho - \omega$ mixing, can be written as:

$$F_\pi(q^2) = 1 + \frac{F_V G_V}{f_\pi^2} \frac{q^2}{m_\rho^2} B_\rho^{KS}(q^2) \left(1 - \frac{\Pi_{\rho\omega}}{3m_\omega^2} B_\omega^{KS}(q^2) \right), \quad (10)$$

where q^2 is the virtuality of the photon, $f_\pi = 92.4$ MeV and the parameter $\Pi_{\rho\omega}$ describes the ρ - ω mixing. As before a constant width is used for the ω -meson. We also assume that the parameter $\Pi_{\rho\omega}$ is a constant and is related to the branching fraction $Br(\omega \rightarrow \pi^+\pi^-)$:

$$Br(\omega \rightarrow \pi^+\pi^-) = \frac{|\Pi_{\rho\omega}|^2}{\Gamma_\rho \Gamma_\omega m_\rho^2}. \quad (11)$$

As was mentioned above, the value of F_V and G_V , as well as the mass of the ρ and ω mesons (m_ρ and m_ω , correspondingly), the parameter of the ρ - ω mixing $\Pi_{\rho\omega}$ and the width of the ω meson are determined in the input file **cards_fasterd.dat**. The RPT parametrization corresponds to the function **F_pi_rpt**.

Inclusion of the ρ' meson modifies the form factor (10) as

$$F_\pi(q^2) = 1 + \frac{F_V G_V}{f_\pi^2} \frac{q^2}{m_\rho^2} B_\rho^{KS}(q^2) \left(1 - \frac{\Pi_{\rho\omega}}{3m_\omega^2} B_\omega^{KS}(q^2) \right) + \frac{F_{V'} G_{V'}}{f_\pi^2} \frac{q^2}{m_{\rho'}^2} B_{\rho'}^{KS}(q^2). \quad (12)$$

2.3 "Improved" Kühn-Santamaria

In Ref. [20] the pion FF was estimated in the framework of the dual-QCD $_{N_c \rightarrow \infty}$ model. However this model assumes the resonances to be of the zero width. The authors of Ref. [18] included the final width of the ρ^0 and the three lowest excited ρ' states and obtained the following expression for the pion FF

$$F_\pi(q^2) = \sum_{n=0}^3 c_n B_r^{KS}(q^2) + \sum_{n>4} c_n \frac{m_n^2}{m_n^2 - s}. \quad (13)$$

This parametrization for the pion FF is contained in the function **F_pi_ks_new**. The numerical value for the parameters c_n and m_n (the mass of the excited ρ mesons) is taken from Ref. [18].

3 Final state radiation models

Using the underlying symmetry, like gauge invariance, charge-conjugation symmetry of the final particles and the photon crossing symmetry, it is possible to write the FS tensor $M_F^{(\mu\nu)}$, that describes the $\gamma^* \rightarrow \pi^+ \pi^- \gamma$ vertex, in terms of three gauge invariant tensors (see [21] and Ref. [23, 24] therein):

$$\begin{aligned} M_F^{\mu\nu}(Q, k, l) &= \tau_1^{\mu\nu} f_1 + \tau_2^{\mu\nu} f_2 + \tau_3^{\mu\nu} f_3, \\ \tau_1^{\mu\nu} &= k^\mu Q^\nu - g^{\mu\nu} k \cdot Q, \quad l = p_1 - p_2, \\ \tau_2^{\mu\nu} &= k \cdot l (l^\mu Q^\nu - g^{\mu\nu} k \cdot l) + l^\nu (k^\mu k \cdot l - l^\mu k \cdot Q), \\ \tau_3^{\mu\nu} &= s (g^{\mu\nu} k \cdot l - k^\mu l^\nu) + Q^\mu (l^\nu k \cdot Q - Q^\nu k \cdot l). \end{aligned} \quad (14)$$

The model dependence comes in only via the implicit form of the scalar functions f_i (we will call them structure functions).

Thus the FSR and interference ($ISR * FSR$) part to the invariant amplitude squared (4) is

$$\begin{aligned} \overline{|M_{FSR}|^2} = \frac{1}{s^2} & \left[a_{11}|f_1|^2 + 2a_{12}\text{Re}(f_1f_2^*) + a_{22}|f_2|^2 \right. \\ & \left. + 2a_{23}\text{Re}(f_2f_3^*) + a_{33}|f_3|^2 + 2a_{13}\text{Re}(f_1f_3^*) \right], \end{aligned} \quad (15)$$

and

$$\begin{aligned} \text{Re}(\overline{M_{ISR}M_{FSR}^*}) = -\frac{1}{4sq^2} & \left[A_1\text{Re}(F_\pi(q^2)f_1^*) + A_2\text{Re}(F_\pi(q^2)f_2^*) \right. \\ & \left. + A_3\text{Re}(F_\pi(q^2)f_3^*) \right]. \end{aligned} \quad (16)$$

The form for the coefficients a_{ik} and A_i can be found in Ref. [21] Eqs. (17), (26), correspondingly.

Here is the list of the FSR production mechanisms that are included in FASTERD:

$$e^+ + e^- \rightarrow \pi^+ + \pi^- + \gamma \quad \text{Bremsstrahlung process} \quad (17)$$

$$e^+ + e^- \rightarrow \phi \rightarrow (f_0; f_0 + \sigma)\gamma \rightarrow \pi + \pi + \gamma \quad \phi \text{ direct decay} \quad (18)$$

$$e^+ + e^- \rightarrow (\phi; \omega') \rightarrow \rho\pi \rightarrow \pi + \pi + \gamma \quad \text{Double resonance process} \quad (19)$$

$$e^+ + e^- \rightarrow (\rho/\rho') \rightarrow \omega\pi^0 \rightarrow \pi^0 + \pi^0 + \gamma \quad \text{Double resonance process} \quad (20)$$

Thus the total contribution to the functions f_i introduced in (14) is

$$f_i = f_i^{(Brem)} + f_i^{(\phi)} + f_i^{(vect)} \quad (21)$$

In the next section we present the models describing these processes.

3.1 Final state Bremsstrahlung

Usually the combined sQED*VMD model is assumed for the FS Bremsstrahlung process [7,14]. In this case the pions are treated as point-like particles (the sQED model) and the total FSR amplitude is multiplied by the pion form factor $F_\pi(s)$, that is estimated in the VMD model. Unfortunately the sQED*VMD

model is an approximation that is valid for relatively soft photons and it can fail for high energy photons, i.e near the $\pi^+\pi^-$ threshold. In this energy region the contributions to FSR, beyond the sQED*VMD model, can be important. As mentioned in Section 2, RPT is supposed to be an appropriate model to describe the pion-photon interaction in the region about and below 1 GeV and this model is used to estimate the contributions beyond sQED*VMD.

Using the sQED*VMD model the structure functions $f_i^{(Brem)}$ (see Eq.(21)) are

$$f_1^{sQED} = \frac{2k \cdot Q F_\pi(s)}{(k \cdot Q)^2 - (k \cdot l)^2}, \quad f_2^{sQED} = \frac{-2F_\pi(s)}{(k \cdot Q)^2 - (k \cdot l)^2}, \quad (22)$$

$$f_3^{sQED} = 0. \quad (23)$$

In the framework of RPT the result is

$$f_i^{(Brem)} = f_i^{sQED} + \Delta f_i^{RPT}, \quad (24)$$

where

$$\Delta f_1^{RPT} = \frac{F_V^2 - 2F_V G_V}{f_\pi^2} \left(\frac{1}{m_\rho^2} + \frac{1}{m_\rho^2 - s - i\sqrt{s}\Gamma_\rho(s)} \right) - \frac{F_A^2}{f_\pi^2 m_a^2} \left[2 + \frac{(k \cdot l)^2}{D(l)D(-l)} + \frac{(s + k \cdot Q)[4m_a^2 - (s + l^2 + 2k \cdot Q)]}{8D(l)D(-l)} \right], \quad (25)$$

$$\Delta f_2^{RPT} = -\frac{F_A^2}{f_\pi^2 m_a^2} \frac{4m_a^2 - (s + l^2 + 2k \cdot Q)}{8D(l)D(-l)}, \quad (26)$$

$$\Delta f_3^{RPT} = \frac{F_A^2}{f_\pi^2 m_a^2} \frac{k \cdot l}{2D(l)D(-l)}, \quad D(l) = m_a^2 - (s + l^2 + 2kPQ + 4kl)/4. \quad (27)$$

For notations and details of the calculation we refer the reader to [21]. The functions Δf_i^{RPT} are calculated by the subroutine **chpt_rpt** whereas f_i^{sQED} are evaluated in the functions **fsr1_sqed**, **fsr2_sqed**, **fsr3_sqed**.

We would like to mention here that the contribution of any model describing Bremsstrahlung FS process can be conveniently rewritten as in Eq. (24) and in the soft photon limit the results should coincide with the prediction of the sQED*VMD model.

3.2 ϕ direct decay

As it was mentioned in the Introduction, at the DAΦNE energy ($\sqrt{s} = m_\phi = 1.01944$ GeV) the final state $\pi\pi\gamma$ can be produced via the intermediate ϕ meson state. In this section we consider the direct rare decay $\phi \rightarrow \pi\pi\gamma$. As shown in [15,22] this process affects only the form factor f_1 of Eq. (14):

$$f_1^{(\phi)} = \frac{g_{\phi\gamma} f_\phi(s)}{s - m_\phi^2 + im_\phi\Gamma_\phi}. \quad (28)$$

The ϕ direct decay is assumed to proceed through the intermediate scalar meson state: $\phi \rightarrow (f_0 + \sigma)\gamma \rightarrow \pi\pi\gamma$ and its mechanism is described by a single form factor $f_\phi(s)$.

In the input file the different following models can be chosen to describe this decay:

- Non structure model [23]
- Linear sigma model [24]
- Chiral unitary approach [25]
- Achasov kaon loop model [26]
- Achasov kaon loop model with inclusion of the σ meson [27]
- Non structure model that includes both the f_0 and σ mesons [22]

The explicit expression for the factor $f_\phi(s)$ for the first three models can be found in [15]. For the fourth (“Achasov kaon loop”) model the form factor f_ϕ reads:

$$f_\phi^{K^+K^-}(s) = \frac{g_{\phi K^+K^-} g_{f_0\pi^+\pi^-} g_{f_0 K^+K^-}}{2\pi^2 m_K^2 (m_{f_0}^2 - s + \text{Re}\Pi_{f_0}(m_{f_0}^2) - \Pi_{f_0}(Q^2))} I\left(\frac{m_\phi^2}{m_K^2}, \frac{s}{m_K^2}\right) e^{i\delta_B(s)}, \quad (29)$$

where $I(., .)$ is an analytical function [15,28] and the phase $\delta_B(s) = b\sqrt{s - 4m_\pi^2}$, $b = 75^\circ/\text{GeV}$ [27]. The term $\text{Re}\Pi_{f_0}(m_{f_0}^2) - \Pi_{f_0}(s)$ takes into account the finite width corrections to the f_0 propagator [26].

In a refined version of this model which includes the σ meson in the intermediate state [27], the form factor f_ϕ can be written as

$$f_\phi^{K^+K^-}(s) = \frac{g_{\phi K^+K^-}}{2\pi^2 m_K^2} e^{i(\delta_{\pi\pi}(s) + \delta_{KK}(Q^2))} I\left(\frac{m_\phi^2}{m_K^2}, \frac{s}{m_K^2}\right)$$

$$\cdot \sum_{R,R'} g_{RK^+K^-} G_{RR'}^{-1} g_{R'\pi^+\pi^-},$$

where $G_{RR'}$ is the matrix of inverse propagators [27]. Such an extension of the model improves the description of the data at low $m_{\pi\pi}$ and was recently used by KLOE in the fit of $\phi \rightarrow \pi^0\pi^0\gamma$ spectrum [29].

The contribution of the ϕ direct decay is calculated in the subroutines **fph1_bcg**, **fph1_ln**, **fph1_cpt**, **fph1_a4q**, **fph1_a4qs**, **fph1_pac** according to the corresponding model.

3.3 Double resonance contribution

Another mechanism producing the final $\pi\pi\gamma$ state is reported in Eqs. (19), (20).

First we consider the $\phi \rightarrow \rho\pi$ mechanism. In this case the ϕ meson decays in $(\rho^\pm\pi^\mp)$ for the charged channel and in $(\rho^0\pi^0)$ for the neutral one and then $\rho \rightarrow \pi\gamma$. The corresponding contribution to the functions $f_i^{(vect)}$ of Eq. (21) is

$$\begin{aligned} f_1^{\phi\rho} &= \frac{C(s)}{16\pi\alpha} [(k \cdot Q + l^2)(D_\rho(R_+^2) + D_\rho(R_-^2)) + 2k \cdot l(D_\rho(R_+^2) - D_\rho(R_-^2))], \\ f_2^{\phi\rho} &= -\frac{C(s)}{16\pi\alpha} [D_\rho(R_+^2) + D_\rho(R_-^2)], \\ f_3^{\phi\rho} &= \frac{C(s)}{16\pi\alpha} [D_\rho(R_+^2) - D_\rho(R_-^2)], \end{aligned}$$

where

$$C(s) = \frac{\sqrt{4\pi\alpha} g_{\pi\gamma}^\rho g_{\rho\pi}^\phi F_\phi s}{m_\phi^2 - s - im_\phi\Gamma_\phi} \quad (30)$$

and $D_\rho(R) = m_\rho^2 - R - im_\rho\sqrt{R}\Gamma_\rho(R)$, $R_+ = (k + p_1)^2$, $R_- = (k + p_2)^2$. The quantities $g_{\rho\pi}^\phi$, $g_{\pi\gamma}^\rho$ are the coupling constants determining respectively the $\phi \rightarrow \rho\pi$ and $\rho \rightarrow \pi\gamma$ vertexes correspondingly, $F_\phi = \sqrt{\frac{3\Gamma(\phi \rightarrow e^+e^-)}{4\pi\alpha^2 m_\phi}}$.

To make connection with the KLOE analysis [29] we add also the phase of the ω - ϕ meson mixing $\beta_{\omega\phi}$ and the constant factor Π_ρ^{VMD} ⁷.

⁷ Including Π_ρ^{VMD} , in our opinion, rescales the constant $g_{\rho\pi}^\phi$ that cannot be directly determined from any experimental decay width

Thus the coefficient (30) is rewritten as

$$C(s) = \frac{\sqrt{4\pi\alpha} g_{\pi\gamma}^\rho g_{\rho\pi}^\phi F_\phi s}{m_\phi^2 - s - im_\phi\Gamma_\phi} \Pi_\rho^{VMD} e^{i\beta_{\omega\phi}}. \quad (31)$$

In the energy region of DAΦNE also the tail of the excited ω meson can play a role: $\gamma^* \rightarrow \omega' \rightarrow \rho\pi$. The explicit form of this contribution is written similar to (30) and is:

$$C_{\rho\pi}^\omega = \frac{\sqrt{4\pi\alpha} g_{\pi\gamma}^\rho g_{\rho\pi}^{\omega'} F_{\omega'} s}{m_{\omega'}^2 - s - im_{\omega'}\Gamma_\omega}. \quad (32)$$

In the considered energy region Eq. (32) can be approximated by a complex constant $C_{\rho\pi}^\omega$ whose the numerical value is taken from the fit of $\pi^0\pi^0\gamma$ spectrum [29]⁸.

Therefore we have

$$C(s) = \frac{\sqrt{4\pi\alpha} g_{\pi\gamma}^\rho g_{\rho\pi}^\phi F_\phi s}{m_\phi^2 - s - im_\phi\Gamma_\phi} \Pi_\rho^{VMD} e^{i\beta_{\omega\phi}} + C_{\rho\pi}^\omega. \quad (33)$$

For the neutral case the $\gamma^* \rightarrow (\rho/\rho') \rightarrow \omega\pi^0 \rightarrow \pi^0\pi^0\gamma$ reaction contributes as well. As for the $\omega' \rightarrow \rho\pi$ channel we replace the explicit expression

$$C_{\omega\pi}^\rho = \frac{\sqrt{4\pi\alpha} g_{\pi\gamma}^\omega g_{\omega\pi}^{\rho'} F_{\rho'} s}{m_{\rho'}^2 - s - im_{\rho'}\Gamma_{\rho'}} + \frac{\sqrt{4\pi\alpha} g_{\pi\gamma}^\omega g_{\omega\pi}^\rho F_\rho s}{m_\rho^2 - s - im_\rho\Gamma_\rho} \quad (34)$$

by a complex constant $C_{\omega\pi}^\rho$, which is again taken from the fit. Then the contribution of the $\gamma^* \rightarrow (\rho/\rho') \rightarrow \omega\pi^0 \rightarrow \pi^0\pi^0\gamma$ mechanism to the functions $f_i^{(vect)}$ is

$$\begin{aligned} f_1^{\rho\omega} &= \frac{C_{\omega\pi}^\rho}{16\pi\alpha} [(k \cdot Q + l^2)(D_\omega(R_+^2) + D_\omega(R_-^2)) + 2k \cdot l(D_\omega(R_+^2) - D_\omega(R_-^2))], \\ f_2^{\rho\omega} &= -\frac{C_{\omega\pi}^\rho}{16\pi\alpha} [D_\omega(R_+^2) + D_\omega(R_-^2)], \\ f_3^{\rho\omega} &= \frac{C_{\omega\pi}^\rho}{16\pi\alpha} [D_\omega(R_+^2) - D_\omega(R_-^2)]. \end{aligned}$$

⁸ Also if we suppose that the direct decay $\gamma^* \rightarrow \rho\pi \rightarrow \pi\pi\gamma$ takes place it contributes to $C_{\rho\pi}^\omega$.

Finally the total contribution is

$$f_i^{(vect)} = f_i^{(\phi\rho)} e^{i\delta_\rho} + c f_i^{(\rho\omega)}, \quad (35)$$

where $c = 1$ for the neutral final state and $c = 0$ for the charged one. We include also an additional phase between the double resonance and ϕ direct contributions (δ_ρ).

The subroutine **rhotopig** calculates the contribution for the double resonance mechanism.

4 Comparison of MC results with analytical prediction. Discussion of the results

For the full angular range $0^\circ < \theta_\gamma; \theta_\pi < 180^\circ$ it is possible to obtain the analytical expression of the cross section for the processes (1) and (2). Here we present the results for the charged final state⁹.

The ISR cross section is

$$\frac{d\sigma^{(ISR)}}{dq^2} = \frac{\alpha(s^2 + q^4)}{3s^2q^2(s - q^2)} |F_\pi(q^2)|^2 \left(1 - \frac{4m_\pi^2}{q^2}\right)^{3/2} (L - 1), \quad L = \ln \frac{s}{m_e^2}, \quad (36)$$

whereas for the FSR process we have

$$\frac{d\sigma^{(FSR)}}{dq^2} = \frac{\alpha^3(s - q^2)}{24\pi s^3} (2h_1 - sh_2), \quad (37)$$

where the form of the functions h_i and the equations to calculate them using the functions f_i can be found in Ref. [21]. For example, in the case of sQED

$$2h_1 - sh_2 = \frac{16\pi\xi|F_\pi(s)|^2}{(kQ)^2} \left[(kQ)^2 + \left(\frac{s}{4} - m_\pi^2\right) (-q^2 + (q^2 - 2m_\pi^2)L_1) \right] \quad (38)$$

with $\xi = \sqrt{1 - \frac{4m_\pi^2}{q^2}}$ and $L_1 = \frac{1}{\xi} \ln \frac{1 + \xi}{1 - \xi}$.

⁹ For the $\pi^0\pi^0\gamma$ case the contribution both from the ϕ direct decay and the double resonance vector mechanism is a half of the corresponding one for the $\pi^+\pi^-\gamma$ final state (except for the $\gamma^* \rightarrow \rho \rightarrow \omega\pi$ case that appears only for the $\pi^0\pi^0\gamma$ FS).

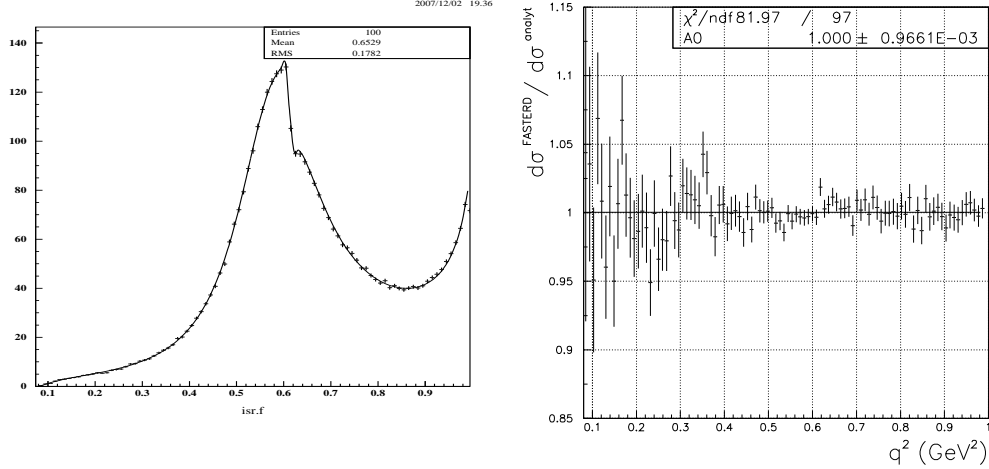


Fig. 2. Comparison of the analytical and numerical results for ISR: $0^\circ < \theta_\pi < 180^\circ$, $0^\circ < \theta_\gamma < 180^\circ$. Left: the solid line corresponds to the analytical result whereas the points with errors have been obtained by FASTERD. Right: the ratio between the analytical results and numerical ones is fitted by the constant A_0 .

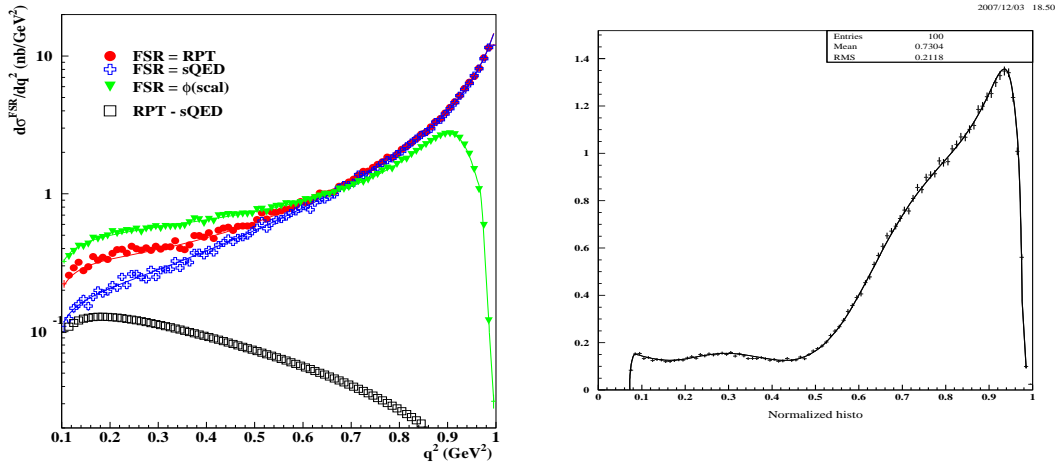


Fig. 3. Comparison of the analytical and numerical results for different contributions to FSR: $0^\circ < \theta_\pi < 180^\circ$, $0^\circ < \theta_\gamma < 180^\circ$. For the ϕ direct decay the kaon loop model with $f_0 + \sigma$ is chosen whereas the RPT parametrization is chosen for the pion FF. The solid lines correspond to the analytical result whereas the points (triangles, squares) have been obtained by FASTERD.

In Figs. 2 and 3 we compare the analytical predictions (36) and (37) with the numerical results obtained by FASTERD for the cross section of the reaction $e^+e^- \rightarrow \pi^+\pi^-\gamma$. The ratio between the analytical and numerical results is fitted by the constant A_0 . We have good χ^2 and the value of A_0 compatible with one.

An important feature of FASTERD is a possibility to estimate the double resonance contribution. At the first sight in the energy region about $s \approx m_\phi^2$ it is enough to include only the $\gamma^* \rightarrow \phi \rightarrow \rho\pi \rightarrow \pi\pi\gamma$ mechanism. However, at $s = m_\phi^2$ our simulation gives the $\sigma(\phi \rightarrow ((f_0 + \sigma)\gamma + \rho^0\pi^0) \rightarrow \pi^0\pi^0\gamma) =$

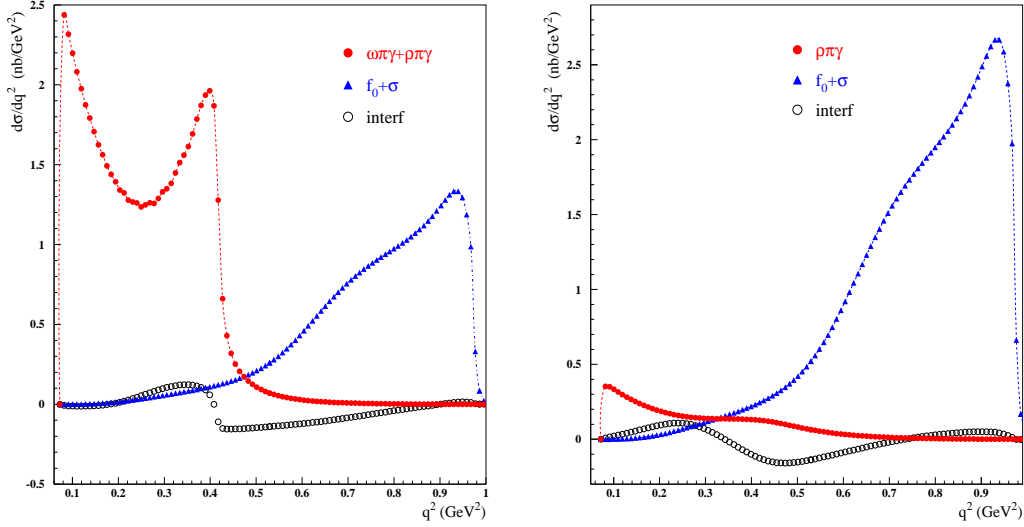


Fig. 4. Different contributions to FSR for the $\pi^0\pi^0\gamma$ (left) and $\pi^+\pi^-\gamma$ (right) final states: $0 < \theta_\pi < 180^\circ$, $0 < \theta_\gamma < 180^\circ$. The filled circles are for the double resonance contribution, the triangles correspond to the $(f_0 + \sigma)\gamma$ mechanism and the empty circles correspond to the interference term between the $(f_0 + \sigma)\gamma$ and the double resonance contributions.

0.451 ± 0.001 nb whereas $\sigma((\rho/\rho') \rightarrow \omega\pi^0 \rightarrow \pi^0\pi^0\gamma) = 0.529 \pm 0.012$ nb (in agreement with KLOE results [30]). In the case of the $\pi^+\pi^-\gamma$ the double resonance mechanism (only the $\phi \rightarrow \rho^\pm\pi^\mp$ contributes) does not give a large contribution in the high q^2 region whereas it gives visible the cross section in the low q^2 region (Fig. 4, right). In the current version FASTERD allows to simulate the processes (1) and (2) for $s \approx m_\phi^2$. To simulate the processes for lower (upto the threshold) and higher (say upto 1.2 GeV^2) energies the exact value of the constants $C_{\rho\pi}^\omega$ and $C_{\rho\pi}^\rho$ (Eq. (32) and Eq. (34)) has to be used.

We compare the ISR spectrum with the results from PHOKHARA [14]. The 'improved' Kühn-Santamaria parametrization was chosen for the pion form factor and PHOKHARA was run at the leading order approximation (only one photon is radiated). The results of comparison are presented in Fig. 5. There the ratio between FASTERD and PHOKHARA results is fitted by the constant A_0 . As one can see the PHOKHARA result coincides with the FASTERD prediction. As it was discussed in Ref. [14] the radiative corrections due to an additional photon emitted by the leptons are relevant and we are planning to include them in the code. An additional photon can be emitted either from initial state or from final state. Inclusion of the second photon emitted from the initial state radiation is a technical task and can be obtained by replacing the leptonic tensor (it has been calculated already [14,21]) and substitution $k \rightarrow k'$, $Q \rightarrow Q' = p_+ - p_- - k'$ in Eq. (14), where k' is the energy of the additional photon emitted from the initial state. Also the one photon phase space has to be replaced to the two photon phase space. For the second

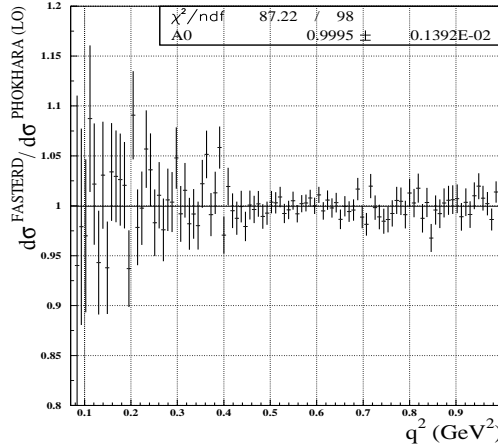


Fig. 5. Comparison of the numerical results for ISR simulated by FASTERD and PHOKHARA : $0 < \theta_\pi < 180^\circ$, $0 < \theta_\gamma < 180^\circ$. The "improved" Kühn-Santamaria parametrization is chosen for the pion FF. The ratio between the numerical results obtained by FASTERD and PHOKHARA is fitted by the constant A_0 .

photon from the final state the situation is more difficult as there is not yet a model-independent calculation for the final state tensors with two photons.

5 The calculation of the spectrum. General algorithm

The logical structure of FASTERD is presented in Fig. 6.

Input parameters are read from the file **cards_fasterd.dat** that is modified by the user (see Appendices A, B for the description of the input file). Here it is possible to choose the name of the output files. The main part of the program runs twice. On the first step, in order to estimate the maximum value of the integrand (M_{max}) some trial events (NMPT) are generated. On the second step (NEVE) events are produced and the acceptance-rejection method is applied to evaluate the cross section $d\sigma/dq^2$. The generator RANMAR [31] is used to generate the random numbers. The variables (q^2 , $\cos\theta_\gamma$, $\cos\phi_\gamma$) are generated in the laboratory frame (e^+e^- center of mass system), the variables ($\cos\theta_\pi^\pm$ and $\cos\phi_\pi^\pm$) are generated in the pion mass reference system. They are calculated in the subroutines **qquadrat** and **photonangles**. The subroutine **vectorb** transforms the azimuthal and polar angles of pions in the laboratory system. The subroutine **rejection** checks the restrictions imposed by the input file. The matrix squared element is produced inside the function **mat**. Using the value *mat* returned by this function the differential cross section *inte* is computed as $inte = mat * num * jac_pion * jac_phot$, where *num* is a kinematic factor for the cross section, *jac_pion* and *jac_phot* are the replacement factors

(they are calculated in the subroutines **qquadrat** and **photonangles**). The information about the accepted events is stored in the file **output.hbk**. At the end of the generation, the cross section is computed by the ratio of accepted to generated events, and the error is estimated. The information about the number of generated and accepted event as well as the value of the cross section and its error is written in a output file.

Function **mat**. The input for **mat** is the 4-momenta of all particles in the laboratory frame and the type of process (ISR, FSR or both ISR+FSR). According to the type of the process either the subroutine **matr_isr** or **matr_fsr** or **matr_int** are called. They compute the Eqs. (5), (15), (16) presented in this paper.

Subroutine **qquadrat**. The following probe function is used to generate the variables q^2 , $\cos\theta_\pi$ and $\cos\phi_\pi$ (we remind that the angles of the pions are generated in the pion reference system)

$$f(q^2, \cos\theta_\pi) = \frac{1}{s(s-q^2)} + \frac{1}{(q^2 - m_\rho^2)^2 + \Gamma_\rho^2 m_\rho^2} + \frac{1}{s(s-q^2)} \left(\frac{1}{1 - \sqrt{1 - \frac{4m_\pi^2}{s}} \cos\theta_\pi} + \frac{1}{1 + \sqrt{1 - \frac{4m_\pi^2}{s}} \cos\theta_\pi} \right).$$

The polar pion angle is generated uniformly.

It results in the following expression for the *jac-pion*

$$jac_pion = \frac{2\pi V}{f(q^2, \cos\theta_\pi)}, \quad (39)$$

where

$$V = -\frac{2}{s} \ln \frac{s - q_{max}^2}{s - q_{min}^2} + \frac{1}{\Gamma_\rho m_\rho} \left(\arctan \frac{q_{max}^2 - m_\rho^2}{\Gamma_\rho m_\rho} - \arctan \frac{q_{min}^2 - m_\rho^2}{\Gamma_\rho m_\rho} \right) - \frac{1}{s(1 - \sqrt{1 - \frac{4m_\pi^2}{s}})^2 \sqrt{1 - \frac{4m_\pi^2}{s}}} \ln \frac{1 + \sqrt{1 - \frac{4m_\pi^2}{s}}}{1 - \sqrt{1 - \frac{4m_\pi^2}{s}}}.$$

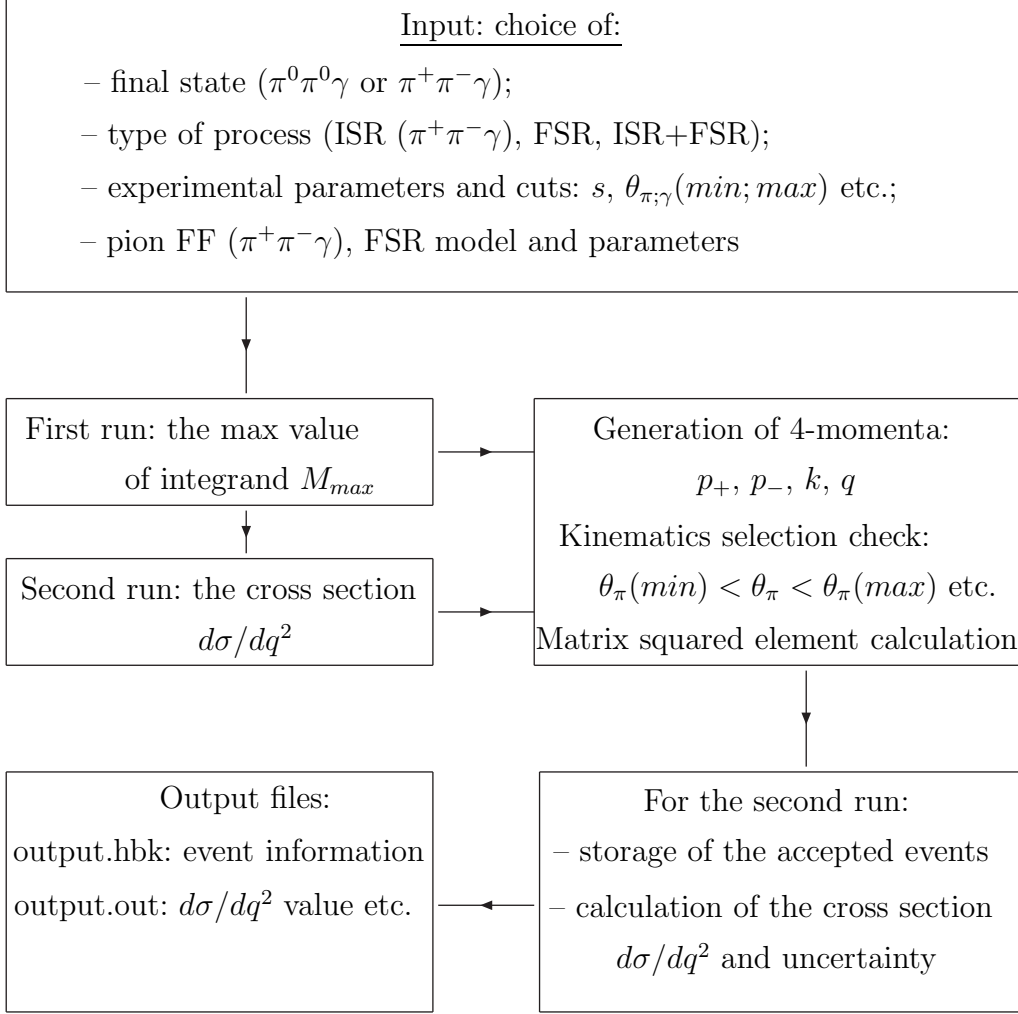


Fig. 6. The logical structure of FASTERD

Acknowledgements

We are grateful to H. Czyż, S. Eidelman, F. Jegerlehner, H. Kühn, and G. Rodrigo, A. Sibidanov and the members of the KLOE collaboration for many useful discussions. G.P. acknowledges support from EU-CT2002-311 Euridice contract. This work has been supported by the grant INTAS/05-100008-8328.

Appendix A. Input file

The main parameters are set in **cards_fasterd.dat** input file. It defines the cuts used in the generation, and the parameters needed for the for the FSR model and the pion FF.

The following variables are included in **cards_fasterd.dat** file:

- NEVE - number of the generated events to be generated
- NPTM - number of events to find the maximum of the cross section.
- NRND - random seed
- FSKIND - kind of final state (FSKIND=0 for $\pi^0\pi^0$ and FSKIND=1 for $\pi^+\pi^-$)
- KIND - two parameters which allows to choose the kind of radiation: (ISR correspond to (1 0), FSR to (0 1) and ISR+FSR to (1 1))
- FPKIND - defines the pion FF parametrization (1 for KS, 2 for GS, 3 for the pion FF in the framework of RPT and 4 for “improved” KS)
- RHOKIND - choice of FSR contribution
- BREMKIND - choice of Bremsstrahlung model
- f0KIND - choice of the model for the ϕ direct decay
- RESPIKIND - allows to choose the intermediate states ($\rho\pi$ and/or $\omega\pi^0$) for the double resonance contribution¹⁰.
- HOUT - defines the name of the output file **output.hbk** where information of the generated particles (4-momenta) is inserted.

The parameters that define the experimental cuts are

- ENES - the squared energy of the initial particles
- GMIN - the minimal energy of the radiated photon
- GMAX - the maximal energy of the radiated photon
- ACUT - the minimal and maximal azimuthal angles of photon and pions

The value of the constants for the pion FF are defined in the arrays *FP* and *FPIHIGH*. The remaining set of arrays *F0par*, *F0fase*, *F0nonstr*, *VMDPAR* defines the numerical values for the ϕ direct decay and the double resonance contribution.

Appendix B. Example of input file

As an example, the input file **cards_fasterd.dat** is set to generate the $e^+e^- \rightarrow \pi^+\pi^-\gamma$ process where:

- the photon is emitted both from IS and FS;
- the RPT parametrization is chosen for the FF;
- FSR is given by sQED Bremsstrahlung and $\phi \rightarrow (f_0 + \sigma)$ decay;
- the experimental cuts are: $50^\circ < \theta_{\pi,\gamma} < 130^\circ$
- the output file is named **isr_rpt_fsr_sqed_f0+sig_50_130_2e6.hbk**

¹⁰ The $\omega\pi$ intermediate state is produced only for the $\pi^0\pi^0$ final state

```

C* --- number of events to be processed
NEVE      1000000
C* --- random seed
NRND      9513463
C* --- number of points used to evaluate the maxima
          (at least 10**4)
NPTM      10000
C* --- pi0pi0 (FSKIND=0) or pi+pi- (FSKIND=1) channel
FSKIND    1
C* --- type of radiation
= (1 1))
C*KIND 1 0    ! initial state radiation on
C*KIND 0 1    ! final   state radiation on
C*KIND 1 1    ! initial+final state radiation
KIND      1 1
C* --- Model for the Pion form factor
C*FPKIND 1  ! KS
C*FPKIND 2  ! GS
C*FPKIND 3  ! RPT
C*FPKIND 4  ! KS+dual-QCD
FPKIND    3
C*FSR --- brems  f0  phirhopi
rhokind   1      1   0
C*bremkind 1  ! sQED
C*bremkind 2  ! RPT
bremkind   1
C*fOKIND  1  ! linear sigma model
C*fOKIND  2  ! non structure model
C*fOKIND  3  ! chiral unitary approach
C*fOKIND  4  ! kaon loop with f0 only
C*fOKIND  5  ! kaon loop with f0+\sigma
fOKIND    5
C*respikind 1 ! only \rho\pi\gamma
C*respikind 2 ! only \omega\pi\gamma
C*respikind 3 ! both \rho\pi\gamma and \omega\pi\gamma
respikind 3
C* --- Parameters of the Pion Form factor
C*RPT MRHO GAMMARHO MRHOL GRHOL MOMEGA GOMEGA AL BE argA
pi\_rho FV FV1 GV1
FP 0.774 0.143 1.37 0.51 0.7827 8.68E-3 0. 0. 0.
-0.0027 0.154 0. 0.
C*FPIHIGH c_0_pion c_2_pion c_3_pion m_rho2_pion g_rho2_pion
m_rho3_pion g_rho3_pion
FPIHIGH 1.171 0.011519 -0.0437612 1.7 0.24 2.0517 0.41
C* --- Parameters of Scalar contribution (f0,f0+sigma) in FSR

```

```

C*F0+SIGMA Gf0\_k+k- Gf0\_p+p- GPHI phase(deg) fOMASS msigma
gsigpp gsigkk Cf0sig
FOPAR 4.02 -1.76 4.482 0. 0.982 415.0e-3 -2.2 -0.37 0.015
C*f0phase F0+SIGMA m0k m2k LambdaK b0p b1p b2p Lambdap
F0fase 0.363 0.757 1.24 5.4 3.7 5.0 0.200
C*F0nonstr gf0_pp gf0_kk gphi_f0g gphi_sgg a0
F0nonstr 0.57 1.14 3.5 5.0e-3 1.
C*----- Parameters of double resonance mechanism
C*VMDPAR g\_rhopig g\_phirpi prhores beta\_bro beta\_wphi
c\_modrpi c\_pharpi c\_modwpi c\_phawpi
VMDPAR 0.295d0 0.811d0 0.677d0 32.996d0 163.0d0
0.26d0 3.1112d0 0.85019d0 0.45d0

C* --- histo output file
*HOUT 'isr_rpt_fsr_sqed_f0+sig_50_130_1e6.hbk'
ENES 1.039202865
GMIN 0.02
GMAX 0.600
C*ACUT theta_min\_gamma theta_max\_gamma theta_min\_pi theta_max\_pi
ACUT 50. 130. 50. 130
C* -----
STOP
END

```

Appendix C. Output file

There are two kinds of output files: (**output.hbk**, HBOOK/PAW ntuple format, defined in **cards_fasterd.dat**) contains the 4-momenta of outgoing particles for each accepted event; (**output.out**, text format, output of the program) contains the number of generated and accepted events, the value of the cross section with the error, and the biggest value of the integrand.

References

- [1] G.W. Bennett *et al.*, Phys. Rev. D **73** (2006) 072003;
James P. Miller, Eduardo de Rafael, B. Lee Roberts, Rep. Prog. Phys. 70 (2007) 795 .
- [2] M. Davier, S. Eidelman, A. Höcker and Z. Zhang, Eur. Phys. J. C **31**(2003) 503;
K. Hagiwara, A. D. Martin, D. Nomura, T. Teubner, Phys. Rev. D **69** (2004)

- 093003;
F. Jegerlehner, Acta Phys. Polon. B **38** (2007) 3021.
- [3] S. Eidelman and F. Jegerlehner, Z. Phys. C **67** (1995) 585.
- [4] W. Kluge, arXiv:hep-ex/0805.4708.
- [5] Min-Shin Chen and P.M. Zerwas, Phys. Rev. D **11** (1975) 58.
- [6] A.B. Arbuzov, E.A. Kuraev, N.P. Merenkov and L. Trentadue, JHEP **12** (1998) 009;
M. Konchatnij and N.P. Merenkov, JETP Lett. **69** (1999) 811.
- [7] S. Binner, J.H. Kühn, K. Melnikov, Phys. Lett. B **459** (1999) 279;(1999) 637;
J. Kühn, Nucl. Phys. B (Proc. Suppl.) **98** (2001) 2.
- [8] V.N. Baier and V.A. Khoze, Sov. Phys. JETP **21** (1965) 629; *ibid.*, **21** (1965) 1145.
- [9] V.A. Khoze, M.I. Konchatnij, N.P. Merenkov *et al.* Eur. Phys. J. C **25** (2002) 199. .
- [10] A. Aloisio *et al.* [KLOE Collaboration], Phys. Lett. B **606** (2005) 12.
- [11] D. Leone, Nucl. Phys. B - Proc. Suppl. **162** (2006) 95.
- [12] G. Pancheri, O. Shekhovtsova and G. Venanzoni, J. Exp. Theor. Phys. **106** (2008) 470;
G. Pancheri, O. Shekhovtsova and G. Venanzoni, Phys. Lett. B **642** (2006) 342.
- [13] H. Czyż, A. Grzelinska and J. H. Kühn, Phys. Lett. B **611** (2005) 116.
- [14] G. Rodrigo H. Czyż, J. H. Kühn and M. Szopa, Eur. Phys. J. C **24** (2002) 71;
H. Czyż, A. Grzelinska, J. H. Kühn and G. Rodrigo, Eur. Phys. J. C **27** (2003) 563;
H. Czyż, A. Grzelinska, J. H. Kühn and G. Rodrigo, Eur. Phys. J. C **33** (2004) 333.
- [15] K. Melnikov, F. Nguyen, B. Valeriani and G. Venanzoni, Phys. Lett. B **477** (2000) 114.
- [16] J. H. Kühn and A. Santamaria, Z. Phys. C **48** (1990) 445.
- [17] G. J. Gounaris, J. J. Sakurai, Phys. Rev. Lett. **21** (1968) 244.
- [18] Ch. Bruch, A. Khodjamirian, J. H. Kühn, Eur. Phys. J. C **39** (2005) 41.
- [19] G. Ecker, J. Gasser, A. Pich and E. de Rafael, Nucl. Phys. B **321** (1989) 311;
G. Ecker, J. Gasser, H. Leutwyler, A. Pich and E. de Rafael, Phys. Lett. B **223** (1989) 425.
- [20] C. A. Dominguez, Phys. Lett. B **512** (2001) 331.
- [21] S. Dubinsky, A. Korchin, N. Merenkov, G. Pancheri and O. Shekhovtsova, Eur. Phys. J. C **40** (2005) 41.

- [22] G. Isidori, L. Maiani, M. Nicolaci and S. Pacetti, JHEP **0605** (2006) 049 .
- [23] A. Bramon, G. Colangelo and M. Greco, Phys. Lett. B **287** (1992) 263.
- [24] J. L. Lucio, M. Napsuciale, Phys. Lett. B **331** (1994) 418.
- [25] E. Marco, S. Hirenzaki, E. Oset, H. Toki, Phys. Lett. B **470** (1990) 20;
J. A. Oller, Phys. Lett. B **426** (1999) 20.
- [26] N. N. Achasov, V. V. Gubin and E. P. Solodov, Phys. Rev. D **55** (1997) 2672;
N. N. Achasov and V. V. Gubin, Phys. Rev. D **57** (1998) 1987.
- [27] N.N. Achasov and A.V. Kiselev, Phys. Rev. D **73** (2006) 054029.
- [28] F. E. Close, N. Isgur and S. Kumano, Nucl. Phys. B **389** (1993) 513.
- [29] F. Ambrosino *et al.* [KLOE Collaboration], Eur. Phys. J. C **49** (2007) 473.
- [30] S. Giovannella, S. Miscetti, KLOE NOTE 212 (2006),
<http://lnf.infn.it/kloe/pub/knote/kn212.ps>;
S. Giovannella, S. Miscetti, KLOE NOTE 213 (2006),
<http://lnf.infn.it/kloe/pub/knote/kn213.ps>.
- [31] CERN Program Library, Library MATHLIB, V113;
F. James, Computer Phys. Comm. **60** (1990) 329.